



A MEANS OF MEASURING SMALL CONCENTRATIONS OF DISSOLVED SUBSTANCES BASED ON A REFRACTOMETRIC SENSOR

Oleksandr Vozniak, Valerii Hraniak
Vinnytsia National Agrarian University

Abstract

Determining the quantitative and qualitative composition of solutes is an important scientific and applied problem that arises in various fields of science and technology. However, in a number of practical problems there is a need to determine the concentration of substances whose mass (volume) fraction in the solution is quite small.

Common measurement methods, characterized by high speed and versatility are refractometric methods. Of particular interest among refractometric methods in the measurement of low concentrations of solutes is the method based on the use of the effect of surface plasmon resonance. The main advantages of this method are its high sensitivity and low weight of the sample used in the study. To date, the widespread use of this method of measurement is significantly limited by the lack of high-precision mathematical models of primary measuring transducers (sensors) implemented on its basis.

The main directions of refractometry development and its relevance in various spheres of human activity, such as science, technology, medicine and even the food industry, were considered in the work. As a result of the need to use the phenomenon of surface-plasmon effect, a detailed description of this phenomenon, its features, nature and practical application. The peculiarity of the interaction of radiation with gold nanofilms is considered.

A mathematical model of the refractometer based on the surface plasmon effect was developed. The adequacy of the obtained conclusions was confirmed by means of computer modeling and experimental research.

The design of a means of measuring small concentrations of dissolved substances, built on the basis of the described sensor, has been developed. It is shown that such a measuring tool will be characterized by relative simplicity of construction while preserving all the advantages of the refractometric measurement method.

Keywords: measurement, concentration, refractometry, surface plasma resonance, refraction.

Received 2024-08-01, accepted 2024-11-01

1. Introduction

Refractometry is used in many fields of science and technology (medicine, industry, field examination, physical research). Thus, when operating a machine and tractor park, the value of the refractive index can be used to determine the quality indicators of fuel and lubricants. In agronomy - to determine the concentration of organic and inorganic components in the prepared substrate, this is introduced during plant processing. In the food industry - to determine the concentration of carbohydrates in various foods, the mass fraction of dry matter, to quantify fats in food, and phase control in the production of food products - confectionery, beverages, some types of canned food, etc. (Palchoudhury *et al.*, 2015). Therefore, based on the above, high-precision rapid determination of the refractive index is of great practical importance as a method of rapid and accurate chemical analysis of matter.

It should also be noted that in solving a number of practical problems it is necessary to determine the concentration of substances whose mass (volume) share in the solution does not exceed 0.1-0.01% (Hu *et al.*, 2011), (Clogston, 2021). And since the detection of such low concentrations of impurities is currently significantly complicated by the low sensitivity of existing sensors, including refractometric, it is obvious that the development of new high-sensitivity sensors and obtaining high-precision mathematical models is of considerable theoretical and practical interest.

2. Setting the Task

The aim of this work is to increase the accuracy of physical models for adequate evaluation of the parameters of surface plasma resonant sensors (SPR sensors).

The realization of this goal required the solution of the following tasks:

1. Improvement of algorithms for solving the inverse problem of determining the optical constants of an ideal multilayer system by measuring the angular spectra of SPR.
2. Determination of quantitative parameters that characterize the adsorption process, the shape and position of the resonance curve.
3. Development of methodological approaches to the assessment of morphological characteristics of interface and multilayer systems using atomic force microscopy, which are used in sensors based on SPR (glass surfaces and semiconductor materials, thin metal films, layers of organic compounds, etc.).
4. Development and approbation of theoretical models to consider the influence of deviations from the ideal morphology of the separation boundary on the SPR spectra

3. Analysis of Methods to Solve the Task

Refractive index n is the ratio of light velocities in adjacent media. For liquids and solids, n is usually determined with respect to air, and for gases with respect to vacuum. In case of gases, dependence between n and pressure must be accounted for. In ideal systems, dependence between refractive index and composition is close to linear, if composition is expressed in volume fractions (percentage) (Hu *et al.*, 2011), (Clogston, 2021).

$$n = n_1 \cdot V_1 + n_2 \cdot V_2, \quad (1)$$

where n , n_1 , n_2 – refractive indices of mixture and components, V_1 and V_2 – volume fractions of components ($V_1 + V_2 = 1$).

For the vast majority of liquids, temperature coefficient lies in the narrow range from -0.0004 to -0.0006 1/deg. Important exceptions are water and dilute aqueous solutions (-0.0001), glycerin (-0.0002) and glycol (-0.00026) (Peatross *et al.*, 2021).

Linear extrapolation of refractive index is permissible for small temperature differences (10° to 20° C). Precise determination of refractive index in wide temperature ranges is carried out using empirical formulae (Razek, 2020).

Devices used to determine refractive indices are called refractometers. Determination is most frequently performed at the temperature of 20° C and wavelength D of sodium atom's spectral line ($\lambda = 589.3$ nm). The refractive index determined under such conditions is designated as n_{20D} . Refractive index measurements are usually performed using Abbe refractometers that operate by determining the angle of total internal reflection when light passes the boundary between two media with different refractive indices. Refractive index measurement ranges from 1.3 to 1.7, the accuracy of determination being $\pm 2 \cdot 10^{-4}$. Less commonly used in practice are Pulfrich refractometers based on measuring the angle of monochromatic light refraction, this ensuring a high accuracy of refractive index determination ($\pm 2 \cdot 10^{-5}$), but requiring a significant amount of investigated solution and light monochromator.

Concentration of substance solutions may be determined using the refractometric method in two ways: calculation-based and graphical. The calculation method uses the formula that reflects the relationship between solution concentration and its refractive index (Hu *et al.*, 2011):

$$n = n_0 + F \cdot C \rightarrow C = \frac{n - n_0}{F}, \quad (2)$$

where n – solution's refractive index; n_0 – solvent's refractive index; F – refractometric factor; C – solution concentration (%).

Refractometric factor (F) demonstrates the change in refractive index when solution concentration is changed by 1%. It is determined experimentally or calculated according to tables of refractive indices. When the graphical method of substance solution concentration determination is used, one builds calibration graph in $n - C$ coordinates, measures the solution's refractive index and finds respective concentration according to the graph.

The refractometric method is used in practice to quantify concentrations of aqueous and non-aqueous solutions, organic and mineral acids, salts, concentrations of ethyl alcohol, glycerol, to determine blood protein content and others.

Developing the Mathematical Model for Refractometric Measurement Device.

To solve this task, the following block diagram of a refractometric measurement device has been developed.

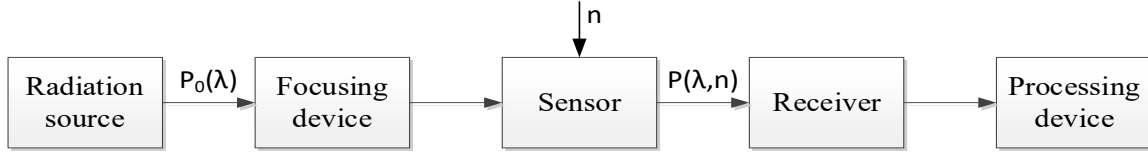


Fig.1. Refractometer's block diagram

The source of non-monochromatic radiation is directed at the focusing device that contains a certain number of lenses to concentrate its light in one beam at the specific point, where studied object is located. Focused light beam is sent to the original measurement transducer (OMT). OMT is a dielectric plate with a nanolayer of gold coating, on the surface of which liquid with measured refractive index is placed. Reflected part of the beam falls on the receiver. Due to the phenomenon of surface plasmon resonance within the gold film, the spectrum of reflected radiation will depend on the refractive index of studied liquid and refractive medium. Obtained data are transmitted to the processing device, where the spectrum is fixed and the wavelength with minimal reflection is determined.

The process of interaction between electromagnetic radiation and metals is described using Maxwell's equations. Radiation frequency and frequency-dependent complex parameter of dielectric constant $\varepsilon(\omega)$ determine the nature of this interaction. Mathematical notation of Maxwell's equation is shown in (3-6) (Dmytruk *et al.*, 2014), (Wenger, 1999):

$$\text{div}D = \rho, \quad (3)$$

$$\text{div}B = 0, \quad (4)$$

$$\text{rot}E = -\frac{\partial B}{\partial t}, \quad (5)$$

$$\text{rot}H = J + \frac{\partial D}{\partial t}. \quad (6)$$

Electric field E (V/m) and magnetic field H (A/m) are related to electric displacement D (C/m²) and magnetic flux density B (Tl) (Hraniak *et al.*, 2018).

$$D = z \cdot z_0 \cdot E, \quad (7)$$

$$B = \mu \cdot \mu_0 \cdot H. \quad (8)$$

Here z and z_0 represent dielectric constant (non-dimensional) and dielectric constant of free space [8,854187817·10⁻¹² F/m], respectively. μ and μ_0 represent magnetic permeability (non-dimensional) and magnetic permeability of free space [4π·10⁻⁷ N/A²], respectively. Let us use Ohm's law to establish the relationship between current value of variable J and electric circuit E (Wenger, 1999):

$$J = \sigma \cdot E. \quad (9)$$

Different models are used to describe frequency dependence between dielectric constant in visible area and nearby ultraviolet range. When characterizing composite structures, the concept of effective dielectric constant is used as mathematical averaging of individual components of bulk metal and the medium, which is described by phenomenological models.

Electromagnetic waves are described by Maxwell's equations common to electromagnetic phenomena. Even in the absence of electric charges and currents in space, Maxwell's equations have nonzero solutions. These solutions describe electromagnetic waves.

Applying *rot* operation to the first two equations, one can obtain separate equations to determine the strength of electric and magnetic fields. These equations have the typical form of wave equations.

From relations (5) and (8) for *rotE* and (6), (7) and (9) for *rotH*, we obtain the following relations:

$$\text{rot}E = -\mu \cdot \mu_0 \cdot \frac{\partial H}{\partial t}, \quad (10)$$

$$\text{rot}H = \sigma \cdot E + \varepsilon \cdot \varepsilon_0 \cdot \frac{\partial E}{\partial t}. \quad (11)$$

Derivation of Fresnel coefficients for metal-coated structures.

Now let's describe the falling wave as

$$E = E_0 e^{i(kr - \omega t)}, \quad \omega = \omega(k), \quad B = \frac{k \cdot E_0}{\omega} e^{i(kr - \omega t)}, \quad (12)$$

reflected wave as

$$E' = R_0 e^{i(k'r - \omega't)}, \quad \omega' = \omega'(k'), \quad B' = \frac{k' \cdot R_0}{\omega'} e^{i(k'r - \omega't)}, \quad (13)$$

and refracted wave as

$$E'' = T_0 e^{i(k''r - \omega''t)}, \quad \omega'' = \omega''(k''), \quad B'' = \frac{k'' \cdot T_0}{\omega''} e^{i(k''r - \omega''t)}. \quad (14)$$

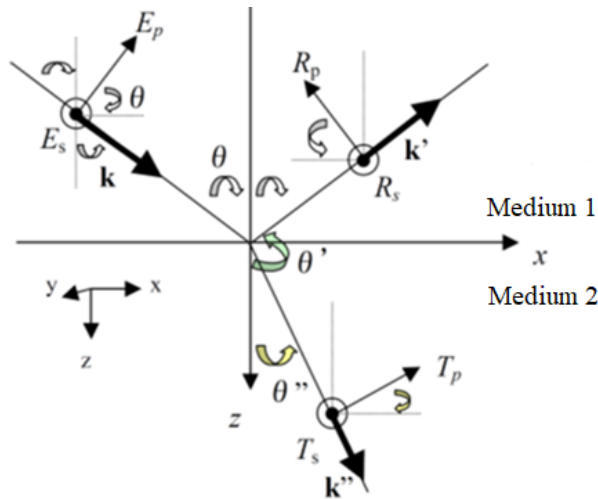


Fig. 2. Light reflection and refraction

Based on Figure 2, we have

$$k = (k \sin \Theta, 0, k \cos \Theta), \quad (15)$$

$$k' = (k' \sin \Theta', 0, k' \cos \Theta'), e^{i(\pi - \Theta')} = -\cos \Theta' + i \cdot \sin \Theta' \quad (16)$$

$$k'' = (k'' \sin \Theta'', 0, k'' \cos \Theta''), \quad (17)$$

p-wave has x and z components, while s-wave has only y component.

Let us introduce condition $t \cdot [E_1 - E_2] = 0$, from which the following expressions for electric field's tangential components will be valid:

$$E_x + E_x' = E_x'' \cdot at \cdot z = 0, \quad (18)$$

$$E_p \cos \Theta \cdot e^{i(k \sin \Theta \cdot x - \omega t)} + R_p \cos \Theta' \cdot e^{i(k' \sin \Theta' \cdot x - \omega' t)} = T_p \cos \Theta'' \cdot e^{i(k'' \sin \Theta'' \cdot x - \omega'' t)}. \quad (19)$$

If introduced condition is fulfilled for any x with $z = 0$, then

$$\omega = \omega' = \omega'', \quad (20)$$

$$k \sin \Theta = k' \sin \Theta' = k'' \sin \Theta''. \quad (21)$$

That said, wave vector value may be obtained from expression

$$k = \frac{2\pi}{\lambda} = \frac{\omega}{v} = \frac{n\omega}{c}. \quad (22)$$

Hence:

$$\sin \Theta = \sin \Theta' = \sin(\pi - \Theta'), \text{ because } k = k'. \quad (23)$$

The incidence angle is equal to the reflection angle, and

$$k \sin \Theta = n_1 \frac{\omega}{c} \sin \Theta = k'' \sin \Theta'' = n_2 \frac{\omega''}{c} \sin \Theta''. \quad (24)$$

Dependence (24) may be reduced to the Snell's law, since $\omega = \omega''$

$$n_1 \sin \Theta = n_2 \sin \Theta''. \quad (25)$$

From (19) we obtain:

$$(E_p - R_p) \cos \Theta = T_p \cos \Theta''. \quad (26)$$

That said, from figure 2 we receive:

$$E_0 = \begin{pmatrix} E_p \cos \Theta \\ E_s \\ -E_p \sin \Theta \end{pmatrix}, R_0 = \begin{pmatrix} -R_p \cos \Theta \\ R_s \\ -R_p \sin \Theta \end{pmatrix}, T_0 = \begin{pmatrix} T_p \cos \Theta'' \\ T_s \\ -T_p \sin \Theta'' \end{pmatrix}. \quad (27)$$

In which case, for the direction parallel to y , the following condition may be entered

$$E_y + E_y' = E_y'' \cdot at \cdot z = 0, \quad (28)$$

$$(E_s + R_s) e^{i(k \sin \Theta'' \cdot x - \omega t)} = T_s e^{i(k'' \sin \Theta'' \cdot x - \omega t)}, \quad (29)$$

$$(E_s + R_s) = T_s. \quad (30)$$

Then for p-wave one can obtain:

$$(E_p - R_s) \cos \Theta = T_p \cos \Theta, \quad (31)$$

$$n_1(E_p + R_s) = n_2 T_p + \frac{\sigma_{12}(k \sin \Theta, \omega)}{\varepsilon_0 n_1 \sin \Theta}, \quad (32)$$

$$\frac{n_1}{\mu_1}(E_p + R_s) = \frac{n_2}{\mu_2} T_p + c \mu_0 [J_s(k \sin \Theta, \omega)]_y. \quad (33)$$

Assuming

$$\begin{cases} \sigma_{12}(k \sin \Theta, \omega) = 0, \\ \text{Im}(n_{1,2}) = 0, \\ \mu_1 = \mu_2 = 1, \\ [J_s(k \sin \Theta, \omega)]_x = 0, \\ [J_s(k \sin \Theta, \omega)]_y = 0. \end{cases} \quad (34)$$

Then for p-wave one can obtain the following ratios:

$$(E_p - R_p) \cos \Theta = T_p \cos \Theta, \quad (35)$$

$$n_1(E_p + R_p) = n_2 T_p. \quad (36)$$

Having determined the amplitude of reflection factor r and the transmission ratio for p-waves' amplitude, we obtain:

$$r_p \equiv \frac{R_p}{E_p}, \quad (37)$$

$$t_p \equiv T \frac{R_p}{E_p}, \quad (38)$$

$$r_s \equiv \frac{R_s}{E_s}, \quad (39)$$

$$t_s \equiv T \frac{R_s}{E_s}, \quad (40)$$

$$(1 - r_p) \cos \Theta = t_p \cos \Theta \quad (41)$$

$$n_1(1 + r_p) = n_2 t_p. \quad (42)$$

From here we obtain Fresnel equation (Khlebtsov, 2008), (Zhu, 2011)

$$r_p = \frac{-n_1 \cos \Theta + n_2 \cos \Theta}{n_1 \cos \Theta + n_2 \cos \Theta}, \quad (43)$$

$$t_p = \frac{2n_1 \cos \Theta}{n_1 \cos \Theta + n_2 \cos \Theta}, \quad (44)$$

$$r_s = \frac{n_1 \cos \Theta - n_2 \cos \Theta}{n_1 \cos \Theta + n_2 \cos \Theta}, \quad (45)$$

$$t_p = \frac{2n_1 \cos \Theta}{n_1 \cos \Theta + n_2 \cos \Theta}. \quad (46)$$

For metal surfaces, optical index becomes complex because some portion of light is absorbed by electronic transition of metal electrons at Fermi level (Zhu, 2011).

$$\underline{n}_2 = n_2 + i \cdot k_2, \quad k'' = \frac{\underline{n}_2 \omega}{c} = (n_2 + i \cdot k_2) \frac{\omega}{c}. \quad (47)$$

Given the assumed condition:

$$n_1 \sin \Theta = \underline{n}_2 \sin \Theta'' = (n_2 + i \cdot k_2) \sin \Theta''. \quad (48)$$

Now θ'' is complex one, determined as

$$\underline{n}_2 \cos \Theta'' \equiv u_2 + i v_2, \quad (49)$$

where u_2 and $i v_2$ are real numbers.

$$(u_2 + i v)^2 = \underline{n}_2^2 \cos^2 \Theta'' = \underline{n}_2^2 \left(1 - \frac{n_1^2}{\underline{n}_2^2} \sin^2 \Theta\right) = \underline{n}_2^2 - n_1^2 \sin^2 \Theta. \quad (50)$$

For real and imaginary parts of equation (49) we have the following definitions

$$u_2^2 - v_2^2 = n_2^2 - k_2^2 - n_1^2 \sin^2 \Theta, \quad (51)$$

$$2u_2 v_2 = 2n_2 n_2. \quad (52)$$

Hence

$$u_2^2 = \frac{n_2^2 - k_2^2 - n_1^2 \sin^2 \Theta + \sqrt{(n_2^2 - k_2^2 - n_1^2 \sin^2 \Theta)^2 + 4n_2^2 k_2^2}}{2}, \quad (53)$$

$$v_2^2 = \frac{-(n_2^2 - k_2^2 - n_1^2 \sin^2 \Theta) + \sqrt{(n_2^2 - k_2^2 - n_1^2 \sin^2 \Theta)^2 + 4n_2^2 k_2^2}}{2}. \quad (54)$$

In view of the foregoing, let us define the equation for refractive index conversion to wavelength with minimal reflection. Such being the case, electronic charges at metal boundary may perform coherent oscillations called surface plasma oscillations. Oscillations are limited at the boundary and disappear on metal surface's both sides. These plasmon waves have p-characteristic, since surface charge induces a break of electric field in surface normal z direction. Reflective power $R_{pr|1|2}$ may be obtained using Fresnel equations in three-layer prism|metal|air system (Zhu, 2011), (Rudenko *et al.*, 2016).

$$r_{ik}^p = \frac{\underline{n}_k \cos \Theta_i - \underline{n}_i \cos \Theta_k}{\underline{n}_k \cos \Theta_i + \underline{n}_i \cos \Theta_k} = \frac{\underline{n}_k \frac{k_{zi}}{k_i} - \underline{n}_i \frac{k_{zk}}{k_k}}{\underline{n}_k \frac{k_{zi}}{k_i} + \underline{n}_i \frac{k_{zk}}{k_k}} = \frac{\underline{\epsilon}_i - \underline{\epsilon}_k}{\underline{\epsilon}_i + \underline{\epsilon}_k}, \quad (55)$$

$$r_{ki}^p = -r_{ik}^p. \quad (56)$$

For refraction (Gunko *et al.*, 2021)

$$t_{ik}^p = \frac{\underline{n}_i}{\underline{n}_k} (1 + r_{ik}^p), \quad (57)$$

$$t_{ki}^p = \frac{\underline{n}_k}{\underline{n}_i} (1 + r_{ki}^p) = \frac{\underline{n}_k}{\underline{n}_i} (1 - r_{ik}^p), \quad (58)$$

$$t_{ki}^p = (1 + r_{ik}^p)(1 + r_{ik}^p). \quad (59)$$

Complete presentation of three-layer system model has the form:

$$R = \left| r_{pr12}^p \right|^2 = \left| \frac{r_{pr1}^p + r_{pr12}^p e^{2ik_z d_1}}{1 + r_{pr1}^p r_{pr12}^p e^{2ik_z d_1}} \right|. \quad (60)$$

Based on (60) we obtain the ratio for the refractometer, according to which the wavelength is defined as the minimum value of optical measurement power in the optical range of:

$$\lambda = \min(P(n, \lambda), \lambda), \quad (61)$$

where,

$$P(n, \lambda) = P_0(\lambda) \cdot R(n, \lambda). \quad (62)$$

To confirm these theoretical results, experimental study was conducted. The experiment was performed using the following initial data:

- the sensitive element represents a dielectric plate of sufficient thickness, on the surface of which a metal layer with the thickness of 30 nm is applied.
- the refraction index ranges from 1.33 to 1.42, as it corresponds to the vast majority of liquid substances.
- liquid layer is large enough to be considered infinite with a permissible error.

Results of physical modeling of functional dependence between wavelength with minimal reflection and liquid's refraction index are shown in Fig. 3.

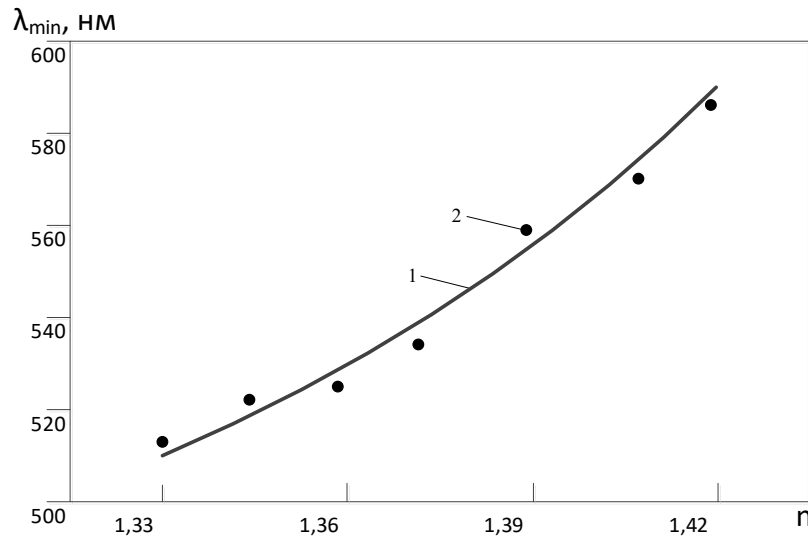


Fig. 3. Dependence between wavelength with minimal reflection and liquid's refraction index: 1 – analytical dependence; 2 – physical modeling results

As follows from Fig. 3, dependence between wavelength with minimal reflection and liquid's refraction index is close to linear, and varies in the wavelength range of 510-580 nm spectrum. This range corresponds to a portion of optical radiation's visible spectrum. That said, the error of mathematical model (61) never exceeds 8%.

Development of the Design of a Means of measuring small concentrations of Dissolved Substances

On the basis of what was said, the design of the means for measuring small concentrations of dissolved substances was developed, which is shown in Fig. 4

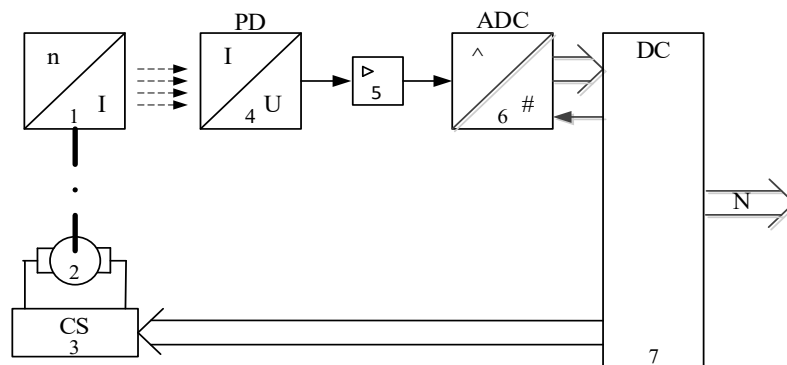


Fig. 4. Structural diagram of a means of measuring small concentrations of dissolved substances

The principle of operation of the measuring device shown in Fig. 4, is as follows. Sensor 1, implemented on the basis of a monochromator, converts the index of refraction of the medium into the intensity of the reflected wave. The change in the wavelength currently used by sensor 1 is realized by turning the dispersive element of the monochromator by servo drive 2, which is controlled by control system 3 on the basis of control signals coming from digital converter 7. The reflected wave from sensor 1 is directed to photoreceiver 4, where it's intensity is converted into a constant voltage level. The constant voltage from the output of the photodetector 4 enters the input of the amplifier 5, where it is amplified and fed to the input of the analog-to-digital converter 6. In the analog-to-digital converter 6, according to the corresponding control signal from the digital converter 7, analog-to-digital conversion of the voltage at its input is carried out and transmission of the received numerical code to the corresponding input of the numerical converter 7. By implementing the described algorithm for different values of the wavelength, the numerical converter 7 determines the wavelength characterized by minimum reflection, and on the basis of the obtained wavelength, the value of the refractive index of the studied sample is determined in accordance with (61).

Conclusions

The main directions of refractometry development and its relevance in various spheres of human activity, such as science, technology, medicine and even the food industry, were considered in the work. As a result of the need to use the phenomenon of surface-plasmon effect, a detailed description of this phenomenon, its features, nature and practical application. The peculiarity of the interaction of radiation with gold nanofilms is considered.

A mathematical model of the refractometer based on the surface-plasmon effect has been developed. A study of the model was conducted, as a result of which it was found that the stability of the power of the radiation source does not affect the measurement error. The adequacy of the obtained conclusions was confirmed by computer modeling and experimental research.

The design of a means of measuring small concentrations of dissolved substances, built on the basis of the described sensor, has been developed. It is shown that such a measuring tool will be characterized by relative simplicity of construction while preserving all the advantages of the refractometric measurement method.

References

- [1] S. Palchoudhury, M. Baalousha, J. R. Lead Methods for Measuring Concentration (Mass, Surface Area and Number) of Nanomaterials. *Frontiers of Nanoscience*, 2015, No 8. P. 153-177. DOI:10.1016/B978-0-08-099948-7.00005-1
- [2] K. Hu, J. J. Ellinger, R. A. Chylla, J. L. Markley Measurement of absolute concentrations of individual compounds in metabolite mixtures by gradient-selective time-zero 1H-13C HSQC with two concentration references and fast maximum likelihood reconstruction analysis. *Analytical Chemistry*, 2011, No 83 (24). 10 p. DOI:10.1021/ac201948f

- [3] J. D. Clogston, The importance of nanoparticle physicochemical characterization for immunology research: what we learned and what we still need to understand. *Advanced Drug Delivery Reviews* 2021, Vol 176. 9 p. 10.1016/j.addr.2021.113897, (113897).
- [4] J. Peatross, M. Ware. 2021. *Physics of Light and Optics*. Brigham: Young University. P. 340
- [5] M. H. A. Razeq Refraction of light and its applications. *Ain Shams Engineering Journal*. 2020, No 31. 13 p.
- [6] M. L. Dmytruk, S. Z. Malynych Surface plasmon resonances and their manifestation in optical properties of nanostructures of precious metals. *Ukrainian Journal of Physics* 2014, Vol. 9, No 1. P. 3-37.
- [7] E. F. Wenger. 1999. *Optics of small particles and dispersed media*. Kyiv: Scientific Opinion. P. 347
- [8] Hraniak V. F., Kukharchuk V. V., Bogachuk V. V., Vedmitskyi Y. G., Vishtak I. V., Popiel P., Yerkeldessova G. 2018. Phase noncontact method and procedure for measurement of axial displacement of electric machine's rotor. *Proc. SPIE 10808, Photonics Applications in Astronomy, Communications, Industry, and High-Energy Physics Experiments* 7 p. DOI:10.1117/12.2501611
- [9] N. G. Khlebtsov Optics and biophotonics of nanoparticles with plasmon resonance. *Quantum Electronics* 2008, Vol. 38, No 6. P. 504-529.
- [10] S. Zhu Optical properties of gold nanoparticles on heavily-doped Si substrate synthesized with an electrochemical process. *Journal of The Electrochemical Society*. 2011, Vol. 158, No 6. P 152–155.
- [11] S. P. Rudenko, L. S. Maksimenko, I. E. Matyash, O. M. Mischuk, M. O. Stetsenko, B. K. Serdega Diagnostic of surface plasmons resonances in nanosized gold films by modulation polarization spectroscopy. *Plasmonics*. 2016, No. 11. P. 557–563.
- [12] I. Gunko, V. Hraniak, V. Yaropud, I. Kupchuk, V. Rutkevych Optical sensor of harmful air impurity concentration. *Przegląd elektrotechniczny*. 2021, No 97(7), P. 76–79. DOI:10.15199/48.2021. 07.15

Author for contacts:

Hraniak Valerii

Vinnitsia National Agrarian University

Soniachna Str. 3, Vinnitsa, Ukraine

E-mail: titanxp2000@ukr.net